

## C<sub>4</sub> Cumulene and the Corresponding Air-Stable Radical Cation and Dication\*\*

Yan Li, Kartik Chandra Mondal, Prinson P. Samuel, Hongping Zhu,\* Claudia M. Orben, Saravanan Panneerselvam, Birger Dittrich,\* Brigitte Schwederski, Wolfgang Kaim,\* Totan Mondal, Debasis Koley,\* and Herbert W. Roesky\*

Dedicated to Professor Hubert Schmidbaur on the occasion of his 80th birthday

**Abstract:** A neutral C<sub>4</sub> cumulene **1** that includes a cyclic alkyl(amino) carbene (cAAC), its air-stable radical cation **1**<sup>•+</sup>, and dication **1**<sup>2+</sup> have been synthesized. The redox property of **1**<sup>•+</sup> was studied by cyclic voltammetry. EPR and theoretical calculations show that the unpaired electron in **1**<sup>•+</sup> is mainly delocalized over the central C<sub>4</sub> backbone. The commercially available CBr<sub>4</sub> is utilized as a source of dicarbon in the cumulene synthesis.

Recent research on species with low-valent elements and main-group radicals has achieved tremendous success by employing an N-heterocyclic carbene (NHC) as a ligand.<sup>[1]</sup> cAAC<sup>[2]</sup> is one of the stable carbenes, which is shown by theoretical calculations to have a singlet spin ground state with a smaller HOMO–LUMO energy gap when compared with NHCs.<sup>[1b,2b,c]</sup> Moreover, recent studies on cAAC show that this molecule is more nucleophilic and also more electrophilic than NHCs.<sup>[2d]</sup> This significantly influences the chemical property of the products. Radicals centered on main-group elements, such as PN<sup>•+</sup>,<sup>[3]</sup> P<sub>2</sub><sup>•+</sup>,<sup>[4]</sup> phosphinyl radical cations,<sup>[5]</sup> H-B<sup>•+</sup>,<sup>[6]</sup> and ketenes with biradical character,<sup>[7]</sup> can be successfully stabilized and isolated by utilizing cAAC. Previously, we reported the syntheses of novel acyclic silylone (cAAC)<sub>2</sub>Si<sup>[8]</sup> and germylone (cAAC)<sub>2</sub>Ge.<sup>[9]</sup> These compounds are the congeners of allenes, which exhibit

biradicaloid character. Furthermore, a (cAAC)<sub>2</sub>(Si<sub>2</sub>Cl<sub>2</sub>) compound was prepared as a silicon analogue of 1,3-butadiene.<sup>[10]</sup> Although cAAC-stabilized silicon and germanium adducts were successfully synthesized, the related chemistry of carbon has not yet been reported.

Carbene-stabilized carbon(0) species, which possess a ylidone structure (C:→:C:←:C), have been experimentally prepared and theoretically analyzed by Bertrand and Frenking et al.<sup>[11]</sup> However, the synthesis of analogous (carbene)<sub>2</sub>C<sub>2</sub> has not been achieved, although compounds (NHC)<sub>2</sub>Si<sub>2</sub><sup>[1a]</sup> and (NHC)<sub>2</sub>Ge<sub>2</sub><sup>[12]</sup> with the sister elements of carbon were documented. Very recently, a Lewis base stabilized dicarbon (C<sub>2</sub>) system has been theoretically predicted,<sup>[13]</sup> which is considered as a terminally functionalized 1,1,4,4-tetraamino C<sub>4</sub>-cumulene.<sup>[14]</sup> The general methods for synthesizing a C<sub>4</sub> unit include metal-mediated C–C coupling of two smaller precursors (C<sub>n</sub> and C<sub>4–n</sub>) or functional transformation of a preformed C<sub>4</sub> unit.<sup>[14a]</sup> Cumulene carbon chains show redox activity when they are connected terminally with transition metals.<sup>[15]</sup> However, their radical species were only detected spectroscopically as unexpected intermediates.<sup>[16]</sup> On the basis of the known carbene chemistry, we were curious to introduce cAAC as a precursor into the synthesis of a cumulene. Herein, we present the isolation of such

[\*] Y. Li, Prof. Dr. H. Zhu  
State Key Laboratory of Physical Chemistry of Solid Surfaces  
College of Chemistry and Chemical Engineering, Xiamen University  
Xiamen, Fujian, 361005 (China)  
E-mail: hpzhu@xmu.edu.cn  
Dr. K. C. Mondal, Dr. P. P. Samuel, C. M. Orben,  
Prof. Dr. H. W. Roesky  
Institut für Anorganische Chemie  
Georg-August-Universität  
Tammannstrasse 4, 37077 Göttingen (Germany)  
E-mail: hroesky@gwdg.de  
Dr. S. Panneerselvam  
Deutsches Elektronen-Synchrotron  
Notke Strasse 85, 22607 Hamburg (Germany)  
Priv.-Doz. Dr. B. Dittrich  
Universität Hamburg  
Martin-Luther-King-Platz 6, 20146-Hamburg (Germany)  
E-mail: birger.dittrich@chemie.uni-hamburg.de

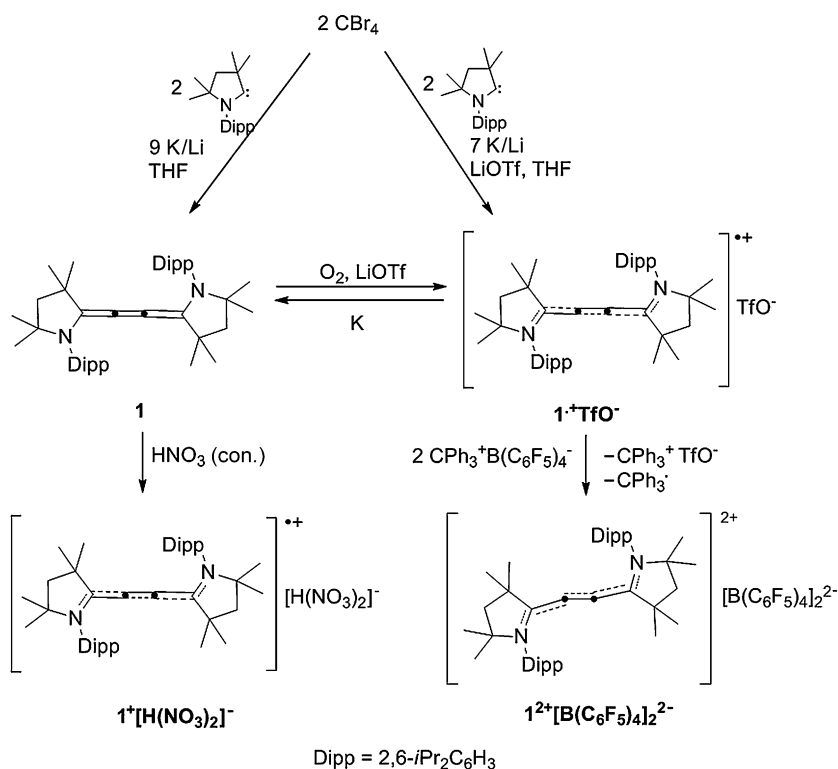
T. Mondal, Dr. D. Koley  
Department of Chemical Sciences  
Indian Institute of Science Education and Research (IISER)  
Kolkata Mohanpur Campus, Mohanpur 741 252 (India)  
E-mail: koley@iiserkol.ac.in  
Dr. B. Schwederski, Prof. Dr. W. Kaim  
Universität Stuttgart, Institut für Anorganische Chemie  
Pfaffenwaldring 55, 70569 Stuttgart (Germany)  
E-mail: kaim@iac.uni-stuttgart.de

[\*\*] H.W.R. acknowledges the Deutsche Forschungsgemeinschaft for financial support (RO 224/60-1). T.M. is thankful to CSIR for the JRF fellowship. D.K. acknowledges IISER-Kolkata for start-up grant and SERB for DST fast track fellowship (SR/FT/CS-72/2011). B.D. acknowledges I. Nevoigt (Universität Hamburg) for the assistance of data collection. Y.L. thanks China Scholarship Council (CSC/91027014) for a fellowship. A part of this work was carried out at the Petral III light source at DESY, a member of the Helmholtz Association (HGF).

Supporting information for this article is available on the WWW under <http://dx.doi.org/10.1002/anie.201310975>.

a cumulene-type dicarbon ( $C_2$ ) species and its redox chemistry.

In an initial experiment, THF was added to a mixture of cAAC (mixed with LiOTf salt),<sup>[2a]</sup>  $CBR_4$ , and K or Li in a molar ratio of 2:2:9 at room temperature, immediately forming a red suspension.<sup>[17]</sup> After vigorously stirring for 48 h, the suspension turned to brown and compound **1** was obtained as yellow crystals from the toluene extract (Scheme 1). Compound **1** is stable in air, even at high temperature. Therefore, a modified method of purification of **1** was developed. The reaction solution was dried and **1** was obtained in 52% yield by sublimation at 240 °C (0.1 mmHg).



**Scheme 1.** Synthesis of cumulene **1** and its conversion into a radical cation and two dications.

Further exploration of an alternative reducing agent ( $KC_8$ ) failed, and the formation of black carbon powder was observed. <sup>1</sup>H and <sup>13</sup>C NMR spectra of **1** clearly exhibit symmetric patterns, showing that both the cAAC units in **1** are equivalent. In the <sup>13</sup>C NMR spectrum of **1**, the resonance ( $\delta = 176.2$  ppm) of the carbene carbons is shifted remarkably upfield when compared with that of cAAC ( $\delta = 304.2$  ppm).<sup>[2a]</sup> The related resonance of the central  $C_2$  is shown at a higher field ( $\delta = 71.2$  ppm). When a similar reaction was carried out utilizing NHC as a carbene source, the analogue of **1** was not obtained. To the best of our knowledge, synthesis of a cumulene employing any carbene has not yet been reported.

Surprisingly, after the separation of **1**, a red crystalline solid was slowly formed as part of the insoluble material, which was filtered and exposed to air along with a small

amount of solvent. The X-ray diffraction analysis showed its  $1^{+\cdot}TfO^-$  structure containing a  $C_4$  cumulene radical cation and a  $TfO^-$  counterion (see the Supporting Information). To confirm this transformation, a mixture of **1** and LiOTf (1:1.2) was stirred overnight in  $CH_2Cl_2$  under exposure to air, and  $1^{+\cdot}TfO^-$  was produced in high yield (Scheme 1). An alternative route to  $1^{+\cdot}TfO^-$  was also developed. The reaction of cAAC (mixed with LiOTf salt),  $CBR_4$ , and K or Li in a molar ratio of 2:2:7 in THF smoothly led to  $1^{+\cdot}TfO^-$  in 87% yield (Scheme 1). A plausible intermediate of this reaction is  $cAAC=C(Br)-C=cAAC$ , which undergoes  $Li^+$ -triggered ionization via  $Br^- \rightarrow TfO^-$  exchange. We envisage that **1** is the reductive product of  $1^{+\cdot}TfO^-$  and both are stepwise formed by debromination of  $CBR_4$ . As expected, reduction of  $1^{+\cdot}TfO^-$  with K exclusively afforded **1**, which was confirmed by NMR analysis.  $1^{+\cdot}TfO^-$  is insoluble in toluene and *n*-hexane, but well-soluble in THF,  $CH_3CN$ , and  $CH_2Cl_2$ , indicating its ionic character. It is thermodynamically stable and has a clear melting point (205 °C). Species  $1^{+\cdot}TfO^-$  is NMR-silent, illustrating its paramagnetic nature. Owing to the insufficient crystallinity of  $1^{+\cdot}TfO^-$ , the quality of the crystal data is limited. However, an X-ray quality crystal of  $1^{+\cdot}TfO^- \cdot THF \cdot H_2O$  was obtained under slow evaporation of the THF solution of  $1^{+\cdot}TfO^-$ ; the corresponding structure is shown in Figure 1.<sup>[18]</sup>

Compound **1** was characterized by X-ray crystallography (Figure 2). The  $C_4$  backbone is centrosymmetric and almost linear. Both the carbene carbon atoms adopt a perfect planar geometry. The C1–C21 (1.3236(16) Å) and C21–C21i (1.249(2) Å) bond lengths, and the C1–C21–C21i angle (178.82(15)°) are comparable to those found in the reported cumulenes and the calculated case.<sup>[14a,13]</sup> In comparison to **1**, the bond lengths of  $1^{+\cdot}TfO^- \cdot THF \cdot H_2O$  change, which is due to the one-electron oxidation. The C1–C21 bond (1.373(4) Å) in  $1^{+\cdot}TfO^- \cdot THF \cdot H_2O$  is slightly elongated, while the C21–C21i bond (1.229(5) Å) is correspondingly shortened. Moreover, the endocyclic C1–N1 bond (1.338(5) Å) in  $1^{+\cdot}TfO^- \cdot THF \cdot H_2O$  is shortened by about 0.04 Å when compared with that in **1** (1.3817(17) Å), indicating the strengthening of the C–N bond that is due to the electron deficiency of the  $C_4$  backbone.

The UV/Vis spectrum of **1** recorded in  $CH_2Cl_2$  shows a weak absorption band at 535 nm, which is quite different from that of  $1^{+\cdot}TfO^-$  (535(s), 495, 466, 408(s), 388 nm).

The EPR spectrum of  $1^{+\cdot}TfO^-$  was recorded in THF solution at room temperature, centered at  $g = 2.0032$ . The relatively small <sup>14</sup>N hyperfine coupling of 5.3 Gauss (quintet 1:2:3:2:1 for two equivalent nitrogen atoms, Figure 3) reflects the concentration of spin on the  $C_4$  backbone with limited participation of the nitrogen centers. This is in agreement with

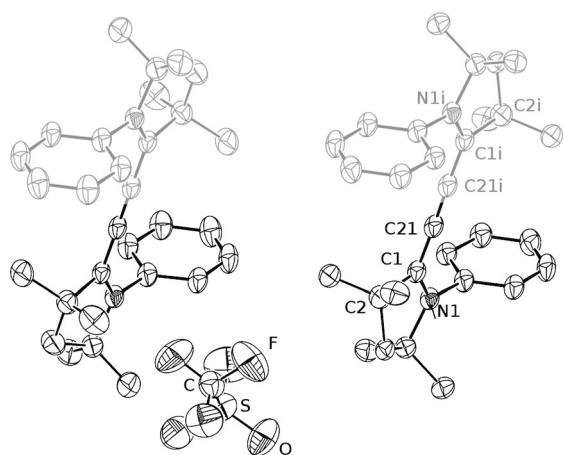


**Figure 1.** Molecular structure of  $1^+ \text{TfO}^- \cdot \text{THF} \cdot \text{H}_2\text{O}$ . Ellipsoids are set at 50% probability; hydrogen atoms, *i*Pr groups, and solvent molecules are omitted for clarity. The second halves of the  $\text{C}_4$  units symmetrically generated are displayed in gray. Only one  $\text{TfO}^-$  is shown. Owing to the essential similarity between the two  $\text{C}_4$  units, selected bond lengths (Å) and angles ( $^\circ$ ) of one labeled  $\text{C}_4$  unit are given (calculated values at the M06-2X/SVP level of theory are listed in square brackets): N1–C1 1.338(5)[1.333], C1–C21 1.373(4)[1.375], C21–C21i 1.229(5)[1.240]; N1–C1–C2 112.08(21)[111.91], C21–C1–N1 123.18(21)[123.13], C21–C1–C2 124.74(24)[124.95], C21i–C21–C1 176.38(26)[178.68].

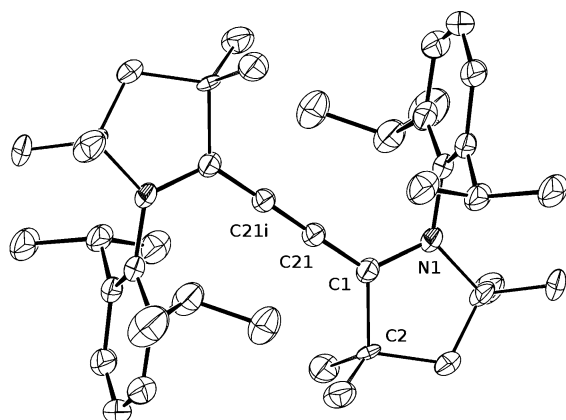


**Figure 2.** Molecular structure of **1**. Ellipsoids are set at 50% probability; hydrogen atoms and solvent molecule (toluene) are omitted for clarity. Selected bond lengths (Å) and angles ( $^\circ$ ) (calculated values at the M06-2X/SVP level of theory are listed in square brackets): N1–C1 1.3817(17)[1.387], C1–C21 1.3236(16)[1.333], C21–C21i 1.249(2)–[1.272]; N1–C1–C2 108.74(28)[109.35], C21–C1–N1 123.87(10)[124.48], C21–C1–C2 127.37(25)[126.14], C21i–C21–C1 178.86(14)[178.80].

structural and computational results (see the Supporting Information). Radical ions of 1,2,3-butatriene were reported but they were only characterized by EPR spectroscopy.<sup>[16]</sup> The coupling of  $^1\text{H}$  with remote substituents is expectedly small and may only contribute to the overall linewidth of two Gauss peak-to-peak difference. The  $^{13}\text{C}$  hyperfine interactions could not be observed as satellites of the main lines and must be smaller than 8 Gauss, in agreement with the DFT calculation.

Compound  $1^+ \text{TfO}^-$  is redox-active and exhibits one reversible one-electron reduction at  $E_{1/2} = -0.313 \text{ V}$  versus  $\text{Fc}^+/\text{Fc}$  in the cyclic voltammogram, which corresponds to

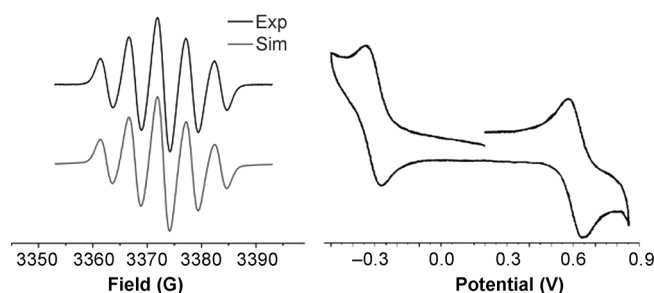


**Figure 3.** Left: X-band EPR spectrum recorded in THF solution at room temperature for  $1^+ \text{TfO}^-$ . ( $g = 2.0032$ ); Right: Cyclic voltammogram for a  $\text{CH}_3\text{CN}$  solution of  $1^+ \text{TfO}^-$ , containing  $0.1 \text{ M } n\text{Bu}_4\text{NPF}_6$  as electrolyte (potential versus  $\text{Fc}^+/\text{Fc}$ , scan rate  $100 \text{ mV s}^{-1}$ ).

$1^+ \rightarrow 1$  (Figure 3). Interestingly, another reversible one-electron oxidation is shown at  $E_{1/2} = 0.608 \text{ V}$ , prompting us to further explore the potential of a dication by employing stronger oxidizing agents.

As anticipated, treatment of **1** with concentrated  $\text{HNO}_3$  successfully produced  $1^{2+}[\text{H}(\text{NO}_3)_2]_2$  as yellow crystals (Scheme 1). An alternative way by the oxidation of  $1^+ \text{TfO}^-$  with  $\text{CPh}_3^+ \text{B}(\text{C}_6\text{F}_5)_4^-$  in  $\text{CH}_2\text{Cl}_2$  also produced the brown-red dication  $1^{2+}[\text{B}(\text{C}_6\text{F}_5)_4]_2$  (see Scheme 1 and the Supporting Information). Both compounds are hardly soluble in organic solvents and show high melting points ( $296$  and  $302$   $^\circ\text{C}$ , respectively). The molecular structure of  $1^{2+}[\text{H}(\text{NO}_3)_2]_2$  is shown in Figure 4.<sup>[19]</sup> On the one hand, the C1–C21 bond ( $1.4367(10) \text{ \AA}$ ) in  $1^{2+}[\text{H}(\text{NO}_3)_2]_2$  is longer than those in **1** and  $1^+$ . On the other hand, the C21–C21i bond ( $1.1855(14) \text{ \AA}$ ) is greatly shortened, which falls in the range of a triple bond. Moreover, the endocyclic C1–N1 bond distance ( $1.2865(9) \text{ \AA}$ ) in  $1^{2+}[\text{H}(\text{NO}_3)_2]_2$  is significantly shorter, by about  $0.05$  and  $0.1 \text{ \AA}$ , than those in **1** and  $1^+$ , respectively. This change indicates the C–N double-bond character that is due to the increase of electron deficiency of the  $\text{C}_4$  backbone.

For a better understanding of the structural, electronic, and redox properties, geometry optimization of **1** was per-

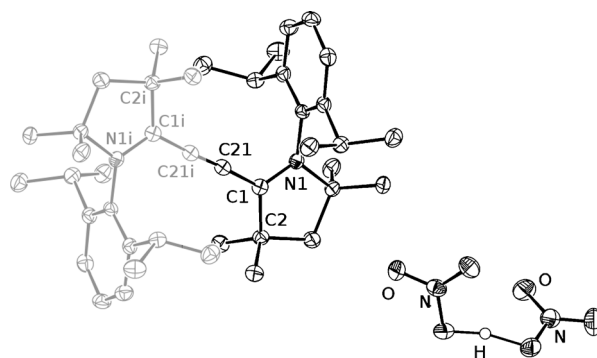


**Figure 4.** Molecular structure of  $1^{2+}[\text{H}(\text{NO}_3)_2]_2$ . Ellipsoids are set at 50% probability; hydrogen atoms in the  $\text{C}_4$  unit are omitted for clarity. The second half of the  $\text{C}_4$  unit which is symmetrically generated is displayed in gray. Only one  $\text{H}(\text{NO}_3)_2^-$  is shown. Selected bond lengths (Å) and angles ( $^\circ$ ) (calculated values at the M06-2X/SVP level of theory are listed in square brackets): N1–C1 1.2865(9)[1.288], C1–C21 1.4367(10)[1.431], C21–C21i 1.1855(14)[1.211]; N1–C1–C2 115.37(7)–[114.61], C21–C1–N1 120.41(7)[121.48], C21–C1–C2 124.22(7)[123.90], C21i–C21–C1 177.58(11)[176.82].

formed at the M06-2X/SVP level of theory.<sup>[20]</sup> Optimizations at both the singlet and triplet states reveal the singlet state to be the electronic ground state with an energy difference ( $\Delta E_{\text{ST}}$ ) of 31.2 kcal mol<sup>-1</sup>. The energy-minimized structures show strong resemblance with the X-ray crystal structure as seen from the alignments and superposition of the respective geometries (Supporting Information, Figure S9).

The HOMO and HOMO-3 of **1** show strong  $\pi$ -interactions along C21-C21i and C1-C21/C21i-C1i bonds with additional electron densities localized on the nitrogen lone pairs (Figure 5 a). A similar electron density distribution was reported by Dutton and Wilson in the DFT study of NHC-

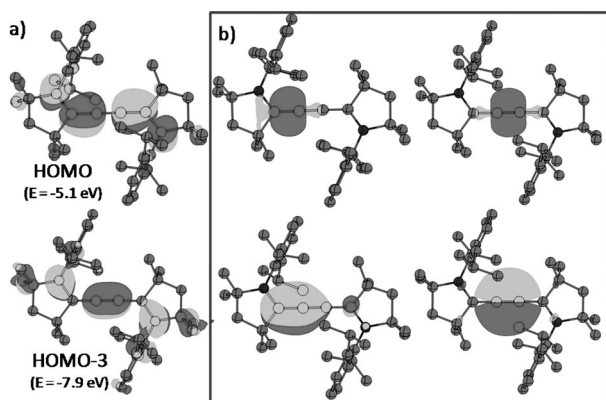


**Figure 5.** a) KS-HOMO and KS-HOMO-3 of **1**; b) Selected NLMOs of **1**. The orbital energies ( $E$ ) are shown in brackets.

stabilized C<sub>2</sub> analogues.<sup>[13a]</sup> Selected natural localized molecular orbitals (NLMOs) of the C21-C21i bond (at M06-2X/TZVP//M06-2X/SVP level) are plotted to emphasize the bonding environment along the C1-C21-C21i-C1i (C<sub>4</sub>) backbone (Figure 5b). The calculated Wiberg bond indices (WBI), at M06-2X/TZVP//M06-2X/SVP level, of C21-C21i and C1-C21/C21i-C1i bonds are 2.07 and 1.62 Å, respectively (Supporting Information, Table S2). The values indicate that both the central C<sub>2</sub> core and the terminal bonds possess double bond character; the former is to a greater extent. Removal of an electron from the HOMO (Figure 5 a) results in the depletion of electron density on the terminal C1-C21/C21i-C1i bonds. This understanding is in agreement with the fact that oxidation of **1** to a radical cation (**1**<sup>+</sup>) results in the elongation of C1-C21/C21i-C1i bond along with the shortening of C21-C21i and N1-C1/N1i-C1i bonds (Supporting Information, Table S2).

M06-2X/SVP optimized structures of the radical cation (**1**<sup>+</sup>) and dication (**1**<sup>2+</sup>) show appreciable difference in geometries, particularly in the central C<sub>2</sub> core and the C-C linkages of cAAC to the C<sub>2</sub> fragment (Supporting Information, Table S2). Under geometry optimizations, both **1**<sup>+</sup> and **1**<sup>2+</sup> undergo an analogous geometry change, resulting in a linear structure similar to that of **1**. There is, however, a very slight decrease in linearity of **1**<sup>2+</sup> with respect to that of **1** (Supporting Information, Table S3). Stronger deviations in bond angles between the solid-state and gas-phase structures are not surprising (Supporting Information, Table S3). A

similar observation was reported by Bestmann et al. in their model phosphonioboratoacetylene species and a possible explanation for such geometrical deviation is due to crystal packing effects.<sup>[21]</sup>

Calculations suggest that the structural deviation of **1**<sup>+</sup> and **1**<sup>2+</sup> with respect to **1** can be explained from the standpoint of lone-pair electron-density depletion on nitrogen atoms and accumulation at the central C<sub>2</sub> core. NBO analysis reveals that in **1**<sup>+</sup> and **1**<sup>2+</sup>, lone pairs are missing on the nitrogen atoms unlike in **1**, indicating that electron density is delocalized to the neighboring C1 center, and N1-C1/N1i-C1i bonds become shorter in the cationic species (Supporting Information, Table S2). Similarly, an opposite trend is observed in C1-C21/C21i-C1i bonds, where we notice that the same bonds are elongated following the trend **1** > **1**<sup>+</sup> > **1**<sup>2+</sup>. With subsequent oxidation of **1** → **1**<sup>+</sup> → **1**<sup>2+</sup>, the electron density on the central C21-C21i bond becomes accumulated as is evidenced from the  $\nabla^2\rho_b$  values (Supporting Information, Table S4), allowing the bond to strengthen (Supporting Information, Table S2). Furthermore, the decrease in  $\epsilon_b$  (Supporting Information, Table S4) for the C1-C21/C21i-C1i and C21-C21i bonds as a consequence of oxidation implies that terminal and central double bonds are transformed to C-C single and triple bonds, respectively, both with higher cylindrical symmetry.<sup>[22]</sup> Based on our calculations, we consider that **1**<sup>+</sup> and **1**<sup>2+</sup> exhibit different resonance structures (Supporting Information, Schemes S2, S3). To evaluate the Lewis basicity of the C<sub>4</sub> species, we have calculated the energies for BH<sub>3</sub> association with **1** and **1**<sup>+</sup> moieties. Formation of the BH<sub>3</sub> adduct **1**·BH<sub>3</sub> is more favorable ( $\Delta G_{298} = 6.2$  kcal mol<sup>-1</sup> for **1** vs. 20.5 kcal mol<sup>-1</sup> for **1**<sup>+</sup>) than **1**<sup>+</sup>·BH<sub>3</sub>.<sup>[13a]</sup> The calculated ionization energies of **1**, **1**<sup>+</sup>, and **1**<sup>2+</sup> are 5.1, 8.8, and 13.5 eV, respectively, which are comparable to those reported in (cAAC)<sub>2</sub>P<sub>2</sub> species.<sup>[4]</sup> Compared to simple butatriene (C<sub>4</sub>H<sub>4</sub>) and other acetylenic compounds, the low first ionization energy of **1** can be attributed to a stable electronic ground state of **1**<sup>+</sup>, having extended delocalization of the positive charge (Supporting Information, Scheme S2).<sup>[16,23]</sup> The calculated hyperfine coupling constant of <sup>14</sup>N atoms in **1**<sup>+</sup> is roughly 3.8 G (Supporting Information, Tables S5, S6), which is relatively close to the experimental value 5.3 G. The computed spin density values unfold the presence of roughly 60% of  $\alpha$ -spin density on the C<sub>4</sub> unit and the rest residing on the N atoms (Supporting Information, Figure S11).

In summary, a novel synthesis of a 1,4-diamino derivative of C<sub>4</sub> cumulene **1** was developed by the reaction of cAAC, CBr<sub>4</sub>, and K or Li. A systematic synthetic study showed that the primitive species **1**<sup>+</sup> forms first, which further undergoes one-electron reduction to form the neutral species **1**. This was further confirmed by cyclic voltammogram, which also suggests the potential approach of a stable dication **1**<sup>2+</sup>. **1**, **1**<sup>+</sup>, and **1**<sup>2+</sup> were synthesized and characterized by X-ray crystallography. The oxidation in the series of **1** → **1**<sup>+</sup> → **1**<sup>2+</sup> results in the increase of the electron density on the central C-C bond with the consequence that this bond is shortened and the terminal C-C bonds are elongated. EPR spectrum of **1**<sup>+</sup> exhibits quintet hyperfine lines, which are originated from the coupling of the radical electron with two equivalent



nitrogen atoms. Both EPR and theoretical calculation indicate that the unpaired electron in  $\mathbf{1}^{+}$  is mainly delocalized over the central  $C_4$  backbone. Moreover,  $\mathbf{1}^{+}\text{TfO}^{-}$  is stable in air, despite it having a radical character.

Received: December 18, 2013  
Published online: March 12, 2014

**Keywords:** cumulenes · cyclic alkyl(amino) carbenes · dications · radical ions · theoretical calculations

- [1] a) Y. Wang, Y. Xie, P. Wei, R. B. King, H. F. Schäfer III, P. von R. Schleyer, G. H. Robinson, *Science* **2008**, *321*, 1069–1071; b) C. D. Martin, M. Soleilhavoup, G. Bertrand, *Chem. Sci.* **2013**, *4*, 3020–3030; c) Y. Wang, G. H. Robinson, *Chem. Commun.* **2009**, 5201–5213.
- [2] a) V. Lavallo, Y. Canac, C. Präsang, B. Donnadiu, G. Bertrand, *Angew. Chem.* **2005**, *117*, 5851–5855; *Angew. Chem. Int. Ed.* **2005**, *44*, 5705–5709; b) D. Martin, M. Melaimi, M. Soleilhavoup, G. Bertrand, *Organometallics* **2011**, *30*, 5304–5313; c) O. Back, M. Henry-Ellinger, C. D. Martin, D. Martin, G. Bertrand, *Angew. Chem.* **2013**, *125*, 3011–3015; *Angew. Chem. Int. Ed.* **2013**, *52*, 2939–2943; d) D. Martin, M. Soleilhavoup, G. Bertrand, *Chem. Sci.* **2011**, *2*, 389–399.
- [3] R. Kinjo, B. Donnadiu, G. Bertrand, *Angew. Chem.* **2010**, *122*, 6066–6069; *Angew. Chem. Int. Ed.* **2010**, *49*, 5930–5933.
- [4] O. Back, B. Donnadiu, P. Parameswaran, G. Frenking, G. Bertrand, *Nat. Chem.* **2010**, *2*, 369–373.
- [5] O. Back, M. A. Celik, G. Frenking, M. Melaimi, B. Donnadiu, G. Bertrand, *J. Am. Chem. Soc.* **2010**, *132*, 10262–10263.
- [6] R. Kinjo, B. Donnadiu, M. A. Celik, G. Frenking, G. Bertrand, *Science* **2011**, *333*, 610–613.
- [7] V. Lavallo, Y. Canac, B. Donnadiu, W. W. Schoeller, G. Bertrand, *Angew. Chem.* **2006**, *118*, 3568–3571; *Angew. Chem. Int. Ed.* **2006**, *45*, 3488–3491.
- [8] a) K. C. Mondal, H. W. Roesky, M. C. Schwarzer, G. Frenking, B. Niepötter, H. Wolf, R. Herbst-Irmer, D. Stalke, *Angew. Chem.* **2013**, *125*, 3036–3040; *Angew. Chem. Int. Ed.* **2013**, *52*, 2963–2967; b) K. C. Mondal, P. P. Samuel, M. Tretiakov, A. P. Singh, H. W. Roesky, A. C. Stückl, B. Niepötter, E. Carl, H. Wolf, R. Herbst-Irmer, D. Stalke, *Inorg. Chem.* **2013**, *52*, 4736–4743.
- [9] Y. Li, K. C. Mondal, H. W. Roesky, H. Zhu, P. Stollberg, R. Herbst-Irmer, D. Stalke, D. M. Andrada, *J. Am. Chem. Soc.* **2013**, *135*, 12422–12428.
- [10] K. C. Mondal, H. W. Roesky, B. Dittrich, N. Holzmann, M. Hermann, G. Frenking, A. Meents, *J. Am. Chem. Soc.* **2013**, *135*, 15990–15993.
- [11] a) C. A. Dyker, V. Lavallo, B. Donnadiu, G. Bertrand, *Angew. Chem.* **2008**, *120*, 3250–3253; *Angew. Chem. Int. Ed.* **2008**, *47*, 3206–3209; b) R. Tonner, G. Frenking, *Angew. Chem.* **2007**, *119*, 8850–8853; *Angew. Chem. Int. Ed.* **2007**, *46*, 8695–8698; c) M. Alcarazo, C. W. Lehmann, A. Anoop, W. Thiel, A. Füstner, *Nat. Chem.* **2009**, *1*, 295–301; d) A. Füstner, M. Alcarazo, R. Goddard, C. W. Lehmann, *Angew. Chem.* **2008**, *120*, 3254–3258; *Angew. Chem. Int. Ed.* **2008**, *47*, 3210–3214.
- [12] A. Sidiropoulos, C. Jones, A. Stasch, S. Klein, G. Frenking, *Angew. Chem.* **2009**, *121*, 9881–9884; *Angew. Chem. Int. Ed.* **2009**, *48*, 9701–9704.
- [13] a) J. L. Dutton, D. J. D. Wilson, *Angew. Chem.* **2012**, *124*, 1506–1509; *Angew. Chem. Int. Ed.* **2012**, *51*, 1477–1480; b) R. I. Kaiser, *Chem. Rev.* **2002**, *102*, 1309–1358; c) W. Weltner, R. J. Van Zee, *Chem. Rev.* **1989**, *89*, 1713–1747.
- [14] a) L. Leroyer, V. Maraval, R. Chauvin, *Chem. Rev.* **2012**, *112*, 1310–1343; b) D. Cremer, E. Kraka, H. Joo, J. A. Stearns, T. S. Zwier, *Phys. Chem. Chem. Phys.* **2006**, *8*, 5304–5316 and references therein; c) R. Chauvin, *Tetrahedron Lett.* **1995**, *36*, 397–400.
- [15] a) P. F. Schwab, M. D. Levin, J. Michl, *Chem. Rev.* **1999**, *99*, 1863–1934; b) F. Paul, W. E. Meyer, L. Toupet, H. Jiao, J. A. Gladysz, C. Lapinte, *J. Am. Chem. Soc.* **2000**, *122*, 9405–9414.
- [16] W. Kaim, H. Bock, *J. Organomet. Chem.* **1979**, *164*, 281–293.
- [17] The reason for the formation of the red color is still not clear. It is perhaps due to the generation of  $\text{CBr}_3$  or Br radicals in the presence of cAAC. See: Q. Kong, M. Wulff, J. H. Lee, S. Bratos, H. Ihee, *J. Am. Chem. Soc.* **2007**, *129*, 13584–13591 and the references therein.
- [18] The calculated molar ratio of  $\text{C}_4^+$  and  $\text{TfO}^-$  anion is 1:1 in the real structure of  $\mathbf{1}^{+}\text{TfO}^{-}\cdot\text{THF}\cdot\text{H}_2\text{O}$ .
- [19] The calculated molar ratio of  $\text{C}_4^+$  and  $\text{H}(\text{NO}_3)_2^-$  anion is 1:2 in the real structure of  $\mathbf{1}^{2+}[\text{H}(\text{NO}_3)_2^-]_2$ .
- [20] Gaussian09 (Revision C.01), M. J. Frisch, et al. Gaussian, Inc., Wallingford CT, **2009**. For full references, see the Supporting Information.
- [21] a) H. J. Bestmann, H. Behl, M. Bremer, *Angew. Chem.* **1989**, *101*, 1303–1304; *Angew. Chem. Int. Ed. Engl.* **1989**, *28*, 1219–1221; b) G. Trinquier, J. P. Malrien, *J. Am. Chem. Soc.* **1987**, *109*, 5303–5315.
- [22] *The Quantum Theory of Atoms in Molecules* (Eds.: C. F. Matta, R. J. Boyd), Wiley-VCH, Weinheim, **2007**.
- [23] F. Brogli, E. Heilbronner, E. Kloster-Jensen, A. Schmelzer, A. S. Manocha, J. A. Pople, L. Radom, *Chem. Phys.* **1974**, *4*, 107–119.